Crystallisation in water-in-cocoa butter emulsions

Di Bari, Vincenzo; Macnaughtan, William; Norton, Jennifer; Sullo, Antonio; Norton, Ian

Link to publication on Research at Birmingham portal

Crystallisation in water-in-cocoa butter emulsions: Role of the dispersed phase on fat crystallisation and polymorphic transition

Vincenzo Di Bari[a,b,c,*], William Macnaughtan[a], Jennifer Norton[c], Antonio Sullo[c], Ian Norton[b,c]

[a] University of Nottingham, Food Sciences, Sutton Bonington Campus, Loughborough, LE12 5RD, United Kingdom
[b] Centre for Innovative Manufacturing in Foods (CIM), United Kingdom
[c] The University of Birmingham, School of Chemical Engineering, Edgbaston, Birmingham, B15 2TT, United Kingdom

ARTICLE INFO

ABSTRACT

The present work is one of the first to focus on the role of emulsified water droplets on the crystallisation behaviour of water-in-cocoa butter emulsions under quiescent conditions (i.e. absence of any externally applied force). Cocoa butter (CB) systems were designed to progressively increase the number of heterogeneous nuclei within the CB matrix, and the crystallisation behaviour was studied at four temperatures ($5\,°C, 10\,°C, 15\,°C$ and $20\,°C$). Information on the crystallisation kinetics and polymorphism was obtained by pulsed nuclear magnetic resonance and differential scanning calorimetry, respectively. This work provides evidence that dispersed water droplets have two key effects on the phase transition of the continuous fat phase: (1) increase the crystallisation rate and (2) enhance the polymorphic evolution. Emulsions crystallised faster (larger Avrami kinetic constant) than the bulk phase at intermediate-low levels of supercooling, although the mechanisms of nucleation did not change across systems. Moreover, at all temperatures, emulsified CB evolved faster towards more stable polymorphs. In these systems, a mechanism of 'interfacial heterogeneous templating' seems unlikely considering that the emulsifier (polyglycerol polyricinoleate) does not crystallise. This result was attributed to the presence of an emulsifier liquid-like layer surrounding the water droplets where the polymorphic evolution could be locally enhanced by the structural re-arrangement of CB triglycerides.

1. Introduction

Water-in-cocoa butter (CB) emulsions represent a novel ingredient developed to reduce the fat content in chocolate (Norton, Fryer, Parkinson, & Cox, 2009). The effect of process and formulation on the microstructure of these emulsions has been described in the literature (Di Bari, Norton, & Norton, 2014; Norton & Fryer, 2012; Sullo, Arellano, & Norton, 2014). Water-in-CB emulsion kinetic stability is provided by both PGPR molecules and fat crystallisation. CB solidification contributes to droplet stability by both network formation and Pickering stabilisation.

Norton and Fryer (2012) were the first to suggest that CB fat crystals contribute to emulsion stability through Pickering stabilisation. The role of CB crystals on emulsion stability was later confirmed by the evidence that stable emulsions could be produced without the addition of PGPR (Di Bari, 2015). In addition, in these systems, the development of a fat crystalline shell surrounding the water droplets was observed, suggesting a mechanism of Pickering stabilisation: the interfacially adsorbed crystals eventually sinter together to form a solid shell. This latter phenomenon implies a process of interfacial crystallisation at the water droplet interface. Although the process of interfacial crystallisation in oil-in-water (O/W) emulsions has been studied in detail, the role of the dispersed phase in fat continuous systems has gained attention only in recent years and remains mostly unknown (Bayés-García et al., 2015). For O/W emulsions, triacyglycerol (TAG) crystallisation behaviour is affected by interfacial layer composition. When high-melting point emulsifiers are at the interface, 'interfacial heterogeneous nucleation' occurs if there are structural similarities between the emulsifiers

and oil TAGs. The presence of a layer of crystalline molecules induces the ordering of the TAGs located near the droplet interface, which results in the formation of different polymorphs compared to bulk fat crystallisation (Douaire et al., 2014). Using a model emulsion system, Ueno et al. (2003) reported the formation of a pseudo-hexagonal crystal form resulting from the interaction between *n*-alkane and additive molecules solidified at the interface. This polymorphic form was not observed in bulk phase with and without the high melting point additives and in O/W emulsions without the same additives. The authors concluded that the solid 'template film' formed by the additive molecules drives the nucleation into the new arrangement by a mechanism of 'interfacial heterogeneous nucleation'. This process may also induce an increase in the nucleation rate (Arima, Ueno, Ogawa, & Sato, 2009; Ueno, Hamada, & Sato, 2003). Less evidence of interfacial local ordering and its effect on fat phase polymorphism is available for W/O emulsions. Saturated monoglycerides have been shown to solidify directly at the interface, which in turn might induce continuous fat phase TAG nucleation by 'interfacial heterogeneous templating' (Ghosh & Rousseau, 2011). The same phenomenon may occur in monomeric liquid surfactant-stabilised droplets in the presence of crystallising bulk TAGs (Rousseau, 2013). Rousseau (2013) has hypothesised that interfacial crystallisation cannot occur for polyglycerol polyricinoleate (PGPR), which was attributed to its liquid physical state and complex interfacial arrangement (not fully elucidated). This arrangement would not allow the necessary TAG–emulsifier interaction and local ordering for interfacial crystallisation to occur. The present study aimed to investigate the crystallisation and polymorphic behaviour of water-in-CB emulsions produced using PGPR as an emulsifier. To the best of our knowledge, this is the first study on the kinetics of crystallisation of water-in-oil (W/O) emulsions. This is because emulsions quickly destabilise when fat is melted (Rousseau, Ghosh, & Park, 2009). In the present study, we showed that water droplets stabilised by PGPR remain stable under quiescent condition even when CB is molten, which offers the opportunity to study the crystallisation behaviour of emulsions. In another recent study, it was shown that freshly produced water-in-CB emulsions stabilised by PGPR remain stable at 50 °C but can destabilise when cooled to freezing temperatures (up to −80 °C) (Rivas, Zelga, Schneider, & Rohm, 2016). The authors also showed that the use of a 50% sucrose solution as dispersed phase resulted in a significant increase in the freeze-thaw stability of emulsions; this result was attributed to higher viscosity and osmotic effects. This study focuses on the polymorphic and crystallisation behaviour of water-in-CB emulsions. It was hypothesised that water droplets would act as seeds promoting CB crystallisation compared to bulk CB. The effect of the interface on the polymorphism of water-in-CB emulsions is more difficult to predict. This is because of the lack of studies investigating the role played by oil-soluble surfactants on the polymorphism of crystallising TAGs in W/O emulsions. To test the hypothesis, the crystallisation behaviour of bulk CB was compared with that of CB enriched with PGPR and of two emulsions containing 19% and 38% (vol%, Φ) aqueous phase. To evaluate the effect of CB system microstructures, samples were melted to erase the crystal memory and crystallised at four temperatures. This allowed the investigation of the combined effect of microstructure and degree of supercooling on CB crystallisation.

The findings of this work are relevant from a fundamental science perspective and for food applications. From an application point of view, the use of water-in-CB emulsions in chocolate manufacture would provide two key advantages: reduced calorie density of the product and evolution towards the desired polymorphic form.

2. Materials and methods

2.1. Materials

The emulsion lipid phase was prepared by blending the appropriate mass of molten CB with PGPR as the emulsifier. The mixing was performed at 60 °C for 15 min. Both ingredients were of standard food grade (Cargill, Vilvoorde, Belgium) and were used without any further purification prior to use. Double distilled water (Aquatron, A4000D, Bibby Scientific Limited, UK) was used as dispersed phase for emulsions.

2.2. Methods

2.2.1. Emulsification

Two emulsion formulations containing 19% and 38% (vol%) dispersed phase were investigated. Emulsions were produced by adding the water to a lipid phase containing 5% PGPR (expressed as weight percentage of the dispersed phase) and using a bench-scale scraped surface heat exchanger (SSHE). The optimised process developed by Di Bari et al. (2014) was used with the following settings: 25 °C for the temperature of the water circulating in the SSHE jacket, 30 mL/min as flow rate for the emulsion circulation through the SSHE and maximum SSHE rotor speed (1315 rpm). As reference materials, bulk CB and CB containing 1% PGPR were crystallised using the same process used for emulsification. After production, all samples were stored in 30-mL sealed plastic pots at 4 °C until analysis. All samples were produced in triplicates.

2.2.2. Droplet size determination

Emulsion droplet size was determined using a benchtop pulsed nuclear magnetic resonance (pNMR) spectrometer (Minispec, Bruker Optics, UK) equipped with a droplet size application. The measurement settings used were selected as reported by Di Bari et al. (2014). The average droplet size expressed as 'Sauter mean diameter' (d_{32}) and free water (i.e. percentage of the dispersed droplets having a diameter of >50 μm) were reported. Measurements were performed in triplicate.

2.2.3. Solid fat content

Isothermal crystallisation of CB systems was investigated using pNMR. Solid fat content (SFC) evolution of the systems was determined with the spectrometer described in Section 2.2.2 using the 'indirect method'. This method relies only on the determination of the point at 70 μs of the free induction decay curve, where the signal decay of the liquid component can be considered negligible and the signal of the solid is less than 0.1% of the original value (Van Putte & Van Den Enden, 1974). A measurement is then performed at a temperature at which all fat is completely melted, and the SFC can be calculated using Eq. (1):

$$SFC(\%) = \frac{c \times S_m - S_L}{c \times S_m} \times 100\% \tag{1}$$

where S_m is the signal produced by the molten fat, S_L is the signal produced by the liquid fraction at the measuring temperature; c is a correction factor that considers the signal loss due to temperature increase on melting. The factor c is calculated from the ratio of the signal intensity of a reference oil (sunflower oil in this study) at working (c_t) and melting temperature (c_m) ($c = c_t/c_m$).

Approximately 0.3 g per sample were weighted into glass tubes (1 mm internal diameter) and heated to 50 °C for 20 min using a dry hot plate to erase crystal memory. The selected sample mass was below the maximum amount required to fill the NMR radio-frequency coil (approximately 1 cm) to prevent any signal loss following thermal expansion on heating. After melting, the samples were transferred into the NMR probe-head (set at the

desired temperature: 5 °C, 10 °C, 15 °C and 20 °C) and readings were started immediately. Data points were acquired every 40 s until SFC curves had achieved a plateau region denoted as maximum (SFC_{max}) (Pérez-Martínez, Alvarez-Salas, Charó-Alonso, Dibildox-Alvarado, & Toro-Vazquez, 2007). At least two sets of data were determined for each sample and averages were reported.

2.2.4. Crystallisation kinetics

To evaluate the effect of sample time–temperature combination on kinetics of crystallisation, data were fitted to the Avrami model. This model describes the change in the fraction of solids over time, and its mathematical expression is given by Eq. (2):

$$(1 - X) = \exp(-k \, t^n) \qquad (2)$$

where X is the fraction of crystallised material during the crystallisation time t and k and n are the *Avrami rate constant* and *exponent*, respectively. The crystal fraction X was expressed here as SFC_t/SFC_{max} with SFC_t and SFC_{max} being the SFC at any time point and at equilibrium, respectively. The parameters k and n were calculated by fitting the data to the linearised form of Eq. (2) obtained by a double logarithmic transformation as expressed in Eq. (3):

$$\ln(-\ln(1 - X)) = \ln(k) + n \ln(t) \qquad (3)$$

2.2.5. Polymorphic evolution of CB systems

In this study, the polymorphic evolution of CB systems was characterised using differential scanning calorimetry (DSC) adopting the 'stop-and-return method' (Foubert, Vanrolleghem, & Dewettinck, 2003; Foubert, Fredrick, Vereecken, Sichien, & Dewettinck, 2008). This method comprises a series of isothermal crystallisation experiments where a molten sample is cooled to the desired annealing temperature and the isothermal hold is interrupted by a re-heating step to gain an insight of the formed polymorphs on annealing. A power-compensated DSC (DSC 8000, PerkinElmer, UK) equipped with an intracooler 2 and controlled by 'Pyris™' software was used. For each sample, a mass corresponding to 4 mg (±1 mg) of CB was weighed in a 40-μL aluminium pan; the pans were then sealed with an aluminium lid and transferred into the DSC furnace. An empty pan was used as reference and dry nitrogen was used to purge the system (20 mL/min). The applied thermal programme consisted of four steps: (1) 5 min of isothermal hold at 50 °C to erase crystal memory (Fessas, Signorelli, & Schiraldi, 2005), (2) cooling to the crystallisation temperature (T_{Cr}) (5 °C, 10 °C, 15 °C and 20 °C) at 10 °C/min to minimise crystallisation on cooling, (3) annealing at crystallisation temperature for 5, 10, 15, 20, 30, 45, 60, 120 and 180 min and (4) re-melting to 50 °C at 5 °C/min. This scan rate was selected as it allows for minimising polymorphic evolution and thermal lag on re-heating (Dewettinck, Foubert, Basiura, & Goderis, 2004; Foubert, Vanrolleghem, & Dewettinck, 2005). For the isothermal steps, following preliminary experiments, the minimum isothermal time was set at 5 min to obtain reproducible signal stability. This is in agreement with the results of Marangoni and Mcgauley (2003), which also referred to the necessity of a minimum isothermal time of 3–4 min for obtaining DSC signal stabilisation.

The heat flow signal (mW) was converted into 'excess of heat capacity' (J/g°C) according to Fessas et al. (2005). From these curves, the enthalpies of melting were calculated using the DSC software. Experiments were performed at least in duplicates for each CB system at all crystallisation temperatures and time points. One limit of the 'stop-and-return method' is that only an estimate of the formed polymorphs can be obtained from the melting peak. To obtain quantitative polymorphic information, endotherms were deconvoluted. The deconvolution analysis was performed

according to the method described by Fessas et al. (2005): each melting curve was divided into a number of Gaussian curves, each of which corresponded to one of the six CB polymorphs. The deconvolution of the endotherms was performed using the 'Solver' tool available in Excel (Microsoft Office, version 2010). The mathematical expression for a Gaussian curve is represented in Eq. (4):

$$y = a \exp\left(-\frac{(x - b)^2}{2c^2}\right) \qquad (4)$$

where a, b and c are three constants representing *height*, *position* and *width* of the curve, respectively. The constants b and c here represent the melting temperature and melting range of each polymorph. To calculate these parameters using the 'Solver' tool, constraints were applied; this preserved the physical differences among polymorphs and restricted the relevant curve to a particular temperature range corresponding to the literature values (Marangoni & Mcgauley, 2003; Van Malssen, Van Langevelde, Peschar, & Schenk, 1999). The melting points and range are shown in Table 1, and an example of the deconvolution analysis is shown in Supplementary Image 1.

The 'relative mass fraction' (expressed in percentage) of each polymorph was calculated from the ratio between the area of the corresponding Gaussian curve and the area of the total deconvoluted experimental endotherm.

2.2.6. Considerations for the isothermal crystallisation behaviour

We studied the effect of PGPR-stabilised water droplets on CB isothermal crystallisation behaviour in terms of both kinetics and polymorphism in bulk and emulsified state. Here, 40 °C is taken as CB final melting temperature (T_m); therefore, the degree of supercooling (ΔT) can be calculated as follows: $\Delta T = T_m - T_{Cr}$.

Kinetic parameters were obtained by Avrami analysis of the crystallisation curves according to the method explained in Section 2.2.4. With respect to CB polymorphism, considering the results of Van Malssen et al. (1999) and Marangoni and Mcgauley (2003), at any temperature between 5 °C and 20 °C, CB is expected to initially crystallise in the α form. The time required for the subsequent monotropic transition to higher polymorphs would depend on the holding temperature and, according to our hypothesis, on the microstructure of the CB systems. Polymorphic evolution is discussed here both in qualitative and quantitative terms. Qualitative information was obtained from the average endotherms and corresponding main melting peaks. The relative mass fraction of polymorphs for all temperatures–samples combinations was calculated using the deconvolution analysis. Given the temperature range investigated, γ polymorph crystallisation (Form I, melting range: from −8 °C to +5 °C) can be excluded; in addition, the presence of Form VI can be ruled out as it is generally produced over periods much longer than those used in

Table 1
Polymorphic form and the corresponding melting peak and range used for the deconvolution analysis*. Melting peak and range correspond to parameters b and c in Eq. (4).

Polymorphic Form	Melting peak temperature (°C) (b parameter)	Melting range (°C) (c parameter)
I or γ	≤ 4	–
II or α	18 ± 2.0	3.0–5.0
III or β'_2	23 ± 1.5	1.0–3.0
IV or β''_1	26 ± 1.5	1.0–3.0
V or β_2	30 ± 1.0	0.5–2.5
VI or β_1	≥ 35	–

*Note: Given the selected experimental conditions, Form I and VI could not be formed (see Section 3.2).

this study (Marangoni & Mcgauley, 2003). Moreover, the expressions 'Form II and α form', 'Form III and β'_2 form' and 'Form IV and β'_1 form' will be used synonymously throughout this manuscript. Finally, it should be noted that an attempt to evaluate the kinetics of polymorphic transformation was made, but it was not successful. The expression 'faster polymorphic transformation' will be used here to indicate a higher amount of more stable form in one sample than in another at the same time point.

3. Results

3.1. Emulsion droplet size

To determine the effect of dispersed phase on the crystallisation properties of water-in-CB emulsions, two emulsified systems were produced. To reduce the number of variables, emulsification parameters were selected to obtain the same final droplet size for both emulsions (Table 2). Therefore, the 38% (vol%) system would contain approximately double the number of seeds (i.e. droplets) within the fat matrix than the 19% (vol%) system, and it is expected to be the fastest to crystallise. A key factor for this study was the stability of emulsion droplets when the CB phase was completely melted. To assess the stability of the systems on heating, emulsions were held at 50 °C for 1 h. As shown in Table 2, emulsions were stable on melting (and re-crystallisation). Although a small increase in the d_{32} and free water content value were noted (together with a decrease in the sigma value), differences were considered negligible. This approximation was made considering that the values of d_{32}, sigma and free water are calculated under the assumption of a monomodal lognormal distribution, with the value of free water representing a fraction of droplets having a large diameter (most likely >15 μm). The decrease in the sigma (i.e. the width of the distribution) value suggests that only some of the larger droplets (>15 μm) may have coalesced during the re-heating step with the smaller ones (representing over 95% of the population of droplets) remaining stable. Furthermore, as discussed in literature (Fredrick et al., 2011), the overlapping of melting and crystallisation curves over multiple cycles also suggests droplet stability (Supplementary Image 2).

3.2. Isothermal crystallisation behaviour

3.2.1. Effect of crystallisation temperature on cocoa butter system solidification

Fig. 1 shows the SFC evolution over time for CB systems crystallised at the four crystallisation temperatures. The dotted lines represent the cooling profile experienced by the samples within the probe as measured with a digital thermometer. No differences in the cooling profiles were observed between samples at each temperature, and for all conditions, the samples reached the crystallisation temperature within 10 min after the start of the experiment. It should be also noted that the thermocouple recorded the temperature evolution at the centre of the sample, i.e. the 'warmest' point of the material. Therefore, it is reasonable to assume that at the wall and in the outer portions of the tubes, samples had reached the desired crystallisation temperature much faster (within 3–4 min). Because the cooling time for the DSC analysis (10 °C/min from 50 °C to the four crystallisation temperatures) ranged from 3 to 4.5 min, the overall cooling time scales for NMR and DSC were considered to be approximately comparable. Therefore, despite the difference in the masses and equipment used, it is reasonable to assume that a qualitative correlation between kinetic evolution of crystalline materials and their polymorphism can be established.

The presence of induction time was observed for none of the crystallisation curves at 5 °C and 10 °C (Fig. 1). This result was attributed to the high level of imposed supercooling (approximately 35–30 °C). The absence of an induction time was also reported for CB at 10 °C by Marangoni and Mcgauley (2003). Furthermore, both the curve shape and SFC$_{max}$ (approximately 88% after 45 min) reported by those authors are very similar to the ones reported in the present study for bulk CB with a SFC$_{max}$ of 90% ± 0.2%. For all samples, the SFC profile increased steeply within the first 20 min of crystallisation, reaching a plateau value above 90% after approximately 30 min. No difference in the SFC content was observed among the systems. The SFC values obtained in the present study for bulk CB are in agreement with that of 90.9% (±1.2%) and 88.8% (±0.8%) reported in the literature (Oliver, Scholten, & Van Aken, 2015).

Values of melting enthalpy are shown in Fig. 2. For all the systems, the measured enthalpy increased over time, indicating increasing extent of crystallisation. At 5 °C, emulsions were characterised by higher melting enthalpies than those recorded for bulk CB at all time points, whereas CB containing 1% PGPR was characterised by intermediate values. It should be noted that the enthalpy of melting for the dispersed system containing 38% aqueous phase was always the highest. Considering that the SFC values were comparable among the systems at 5 °C, the difference in the enthalpies may have resulted from the differences in the polymorphism as suggested by the melting curves shown in Fig. 4 (see Section 3.2.3.1.). When crystallised at 10 °C, the values of melting enthalpy (Fig. 2) recorded in the first 30 min of crystallisation were the same among the systems. At annealing time above 45 min, emulsions were characterised by a higher melting enthalpy, and differences in the enthalpy values were significant only towards the end of the annealing process. This result suggests that CB in emulsions was arranged in a more stable crystalline form than in the bulk state (i.e. non-emulsified).

For the isothermal crystallisation experiment at 15 °C, a small induction time was observed only for bulk CB, which also displayed a less steep increase in the SFC value over time (Fig. 1). However, the SFC$_{max}$ value obtained for bulk CB (90.1% ± 0.4%) is comparable to that recorded for emulsions (92.7% ± 0.2% and 94.2% ± 0.4% for 19% and 38% aqueous phase emulsions, respectively). In their study on CB isothermal crystallisation, Metin and Hartel (1998) reported that complete crystallisation occurs within 35 min

Table 2
Droplet characteristics of emulsions after emulsification and after isothermal hold at 50 °C. The ±limits are the standard deviations of three measurements. However, the difference between the particle size for each emulsion before and after melting may not be significantly different because of the large width of the peaks (sigma value) and the inherent difficulty of calculating this parameter, which reduces the robustness of the estimate (see text for further details).

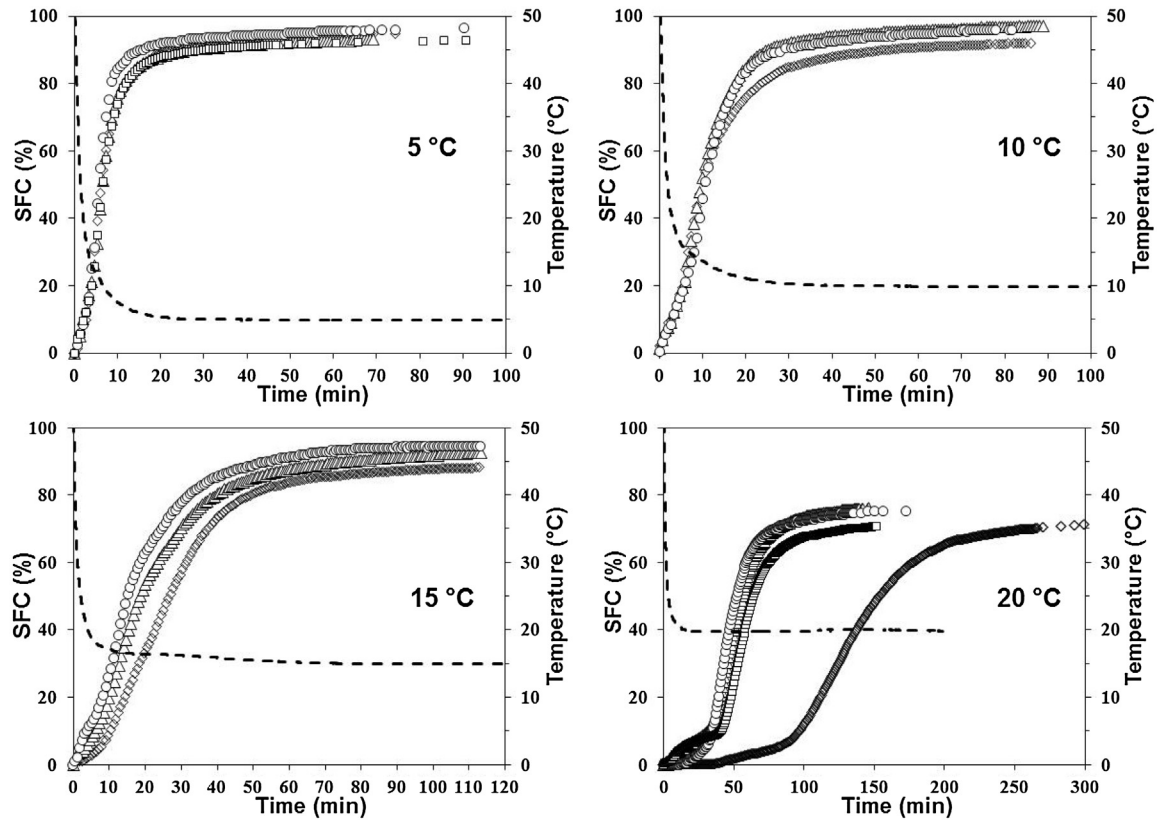| Emulsion system	After emulsification			After melting		
	d_{32} (μm)	Sigma (σ)	Free water (%)	d_{32} (μm)	Sigma (σ)	Free water (%)
19% Aq. phase	2.0 ± 0.11	0.61	0.00	2.8 ± 0.26	0.38	3.4
38% Aq. phase	2.8 ± 0.20	0.44	2.64	3.7 ± 0.37	0.41	3.1

Fig. 1. NMRcrystallisation curves for CB systems at the four isothermal temperatures(reported in each panel). Diamonds, triangles, circles and square symbols represent bulk CB, 20% emulsions, 40% emulsion and CB with 1% PGPR, respectively. Dashed lines represent the cooling profile measured with a thermometer.

(SFC approximately 95%) at 15 °C. In this study, the SFC curve entered the plateau region after approximately 45 min of isothermal holding, with the difference being most likely due to the experimental set-up. Moreover, the SFC_{max} measured here is comparable to that reported by Oliver et al. (2015) (85.9% ± 0.6%) but is considerably more than the 75% reported by Marangoni and Mcgauley (2003). Nevertheless, the general curve shape and the time to reach the plateau region reported by the latter authors are in agreement with those described here.

All crystallisation curves obtained at 20 °C have a sigmoid shape characterised by the presence of an induction time where no solid material is detected (Fig. 1). This step is followed by a rapid increase in the SFC before levelling off to a plateau value. It can be seen from the cooling profile that all the systems had reached the desired temperature within approximately 15 min, i.e. within their induction period. Despite the similar curve shapes, differences can be easily observed among the systems: emulsions were characterised by the smallest induction time (approximately 30 min) and entered the plateau region in a time scale at which the SFC curve of bulk CB was entering its steep increase region (approximately 100 min after the start). Bulk CB achieved its plateau SFC value more than 3 h after the start of the experiment, and both the SFC curve shape and SFC_{max} value (71.0% ± 0.3%) are comparable to those reported by Foubert et al. (2005) (72%) and Dewettinck et al. (2004) (72.5%) but lower than the value of 78.0% ± 0.7% reported by Oliver et al. (2015). Both emulsions had a SFC_{max} of 75.0% ± 0.7% (no difference with bulk CB). The CB system containing 1% PGPR was characterised by an induction time that was comparable to the one recorded for the emulsions. Values of melting enthalpy for the 38% aqueous phase emulsion (Fig. 2) were the highest throughout the annealing time, whereas for the 19% emulsions, differences became significant only at a resting period of above 1 h. No

differences were detected between the bulk CB and CB containing 1% PGPR. These results are in good agreement with SFC data and confirm that crystallisation occurs faster in emulsified systems than in bulk fat. From the initial hypothesis, this behaviour can be explained by considering that water droplets act as seeds within the fat phase, thus accelerating the solidification process when a low supercooling is applied.

3.2.2. Crystallisation kinetics

In this section, we aimed to understand the role of the microstructure of CB systems on the rate of crystallisation (*k* constant) and type of nucleation (*n* constant) of CB using the Avrami model.

3.2.2.1. Crystallisation kinetics at 5 °C and 10 °C. To compare the kinetics of crystallisation among systems, for experiments performed at 5 °C and 10 °C, only the SFC data recorded between 5 and 20 min after the start were used for the Avrami fitting. This was done to compare the kinetics of the α polymorph formation. As discussed in detail in Section 3.2.3.1, the α polymorph is the main form in the early stage of the crystallisation process. Fitting of the SFC data for longer isothermal holding times was not considered as it would have been a function of both further crystallisation and polymorphic evolution. In all cases, fitting of the data to the model yielded good results ($R^2 \geq 0.89$ and 0.995 for all the systems at 5 °C and 10 °C, respectively). Parameters obtained from the Avrami fitting are shown in Table 3. The calculated exponents *n* had a value of approximately 1 for all the systems, suggesting an instantaneous nucleation mechanism, i.e. nuclei appear all at once after reaching the crystallisation temperature (Yang, Hrymak, & Kedzior, 2013). This result is expected considering the high level of imposed
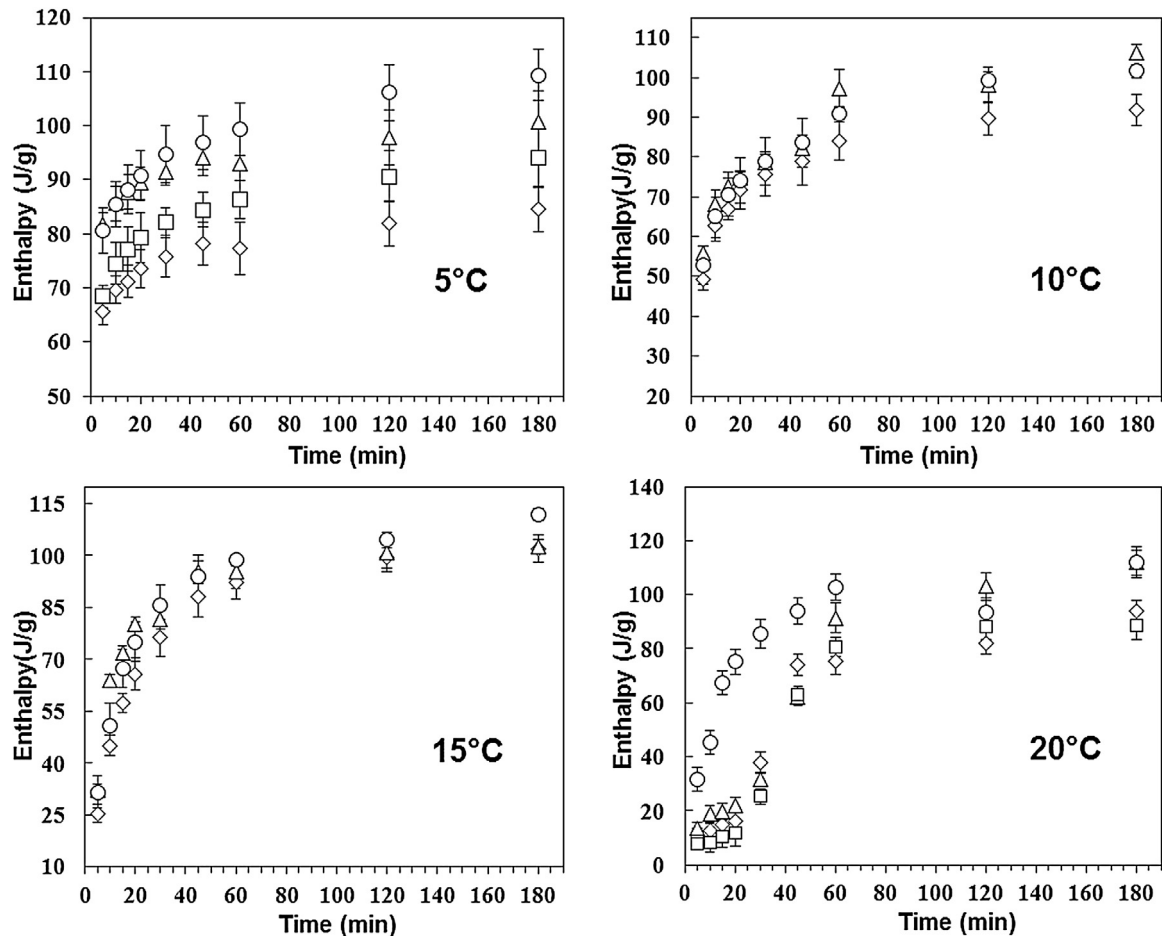
Fig. 2. Meltingenthalpy per gram of fat for CB systems crystallised at the four isothermal temperatures(reported in each panel).Diamonds, triangles, circles and square symbols represent bulk CB, 20% emulsions, 40% emulsion, and CB with 1% PGPR, respectively.

Table 3
Avrami parameters (n and k) and R^2 of the fitting for the SFC data obtained on isothermal crystallisation at all the investigated temperature for CB systems.

Temperature (°C)	Sample	n	k (t^{-n})	R^2
5	CB	1.13	1.0×10^{-2}	0.967
5	19% Aq. Phase	1.29	7.0×10^{-2}	0.929
5	38% Aq. Phase	1.03	1.6×10^{-1}	0.892
5	1% PGPR in CB	1.27	7.0×10^{-2}	0.951
10	CB	1.09	5.0×10^{-2}	0.995
10	19% Aq. Phase	1.40	3.0×10^{-2}	0.998
10	38% Aq. Phase	1.36	6.0×10^{-2}	0.997
15	CB	2.1	8.0×10^{-4}	0.995
15	19% Aq. Phase	1.9	3.3×10^{-3}	0.997
15	38% Aq. Phase	1.9	4.6×10^{-3}	0.992
20	CB	3.83	5.1×10^{-9}	0.998
20	19% Aq. Phase	3.67	4.0×10^{-7}	0.994
20	38% Aq. Phase	4.09	9.3×10^{-8}	0.962
20	1% PGPR in CB	3.63	2.4×10^{-7}	0.979

supercooling (approximately 35 °C–30 °C). The obtained *n* values of bulk CB are in agreement with the ones reported by Marangoni and Mcgauley (2003). The crystallisation rate constant (*k*) is also comparable among the systems, and therefore, the half time of crystallisation ($t_{1/2}$) is the same for all samples (data not shown). These results suggest that the presence of water droplets did not modify the nucleation mechanism and did not produce an increase in the rate of crystallisation at high level of imposed supercoolings.

3.2.2.2. Crystallisation kinetics at 15 °C and 20 °C. We investigated the crystallisation kinetics at low-intermediate levels of degree of supercooling for CB systems with different microstructures. For the crystallisation experiment performed at 15 °C, the SFC data collected between 5 and 20 min of isothermal hold were used to calculate the Avrami parameters of emulsions. For bulk CB, the SFC data between 10 and 25 min were used. The difference in the time range selected for the Avrami analysis was caused because only bulk CB displayed the presence of a short induction time where no crystallisation had occurred. These time ranges (both of 15 min) were selected because they corresponded to linear portions of the curves in a double logarithmic plot and a crystallisation stage where α polymorph was the main form. The SFC data were fit to the Avrami model, and the results are listed in Table 3. For all the systems, the Avrami exponent had a value of approximately 2 (Table 3), suggesting that crystallisation had occurred through an instantaneous nucleation process (this result is discussed in more detail in Section 4.1). The Avrami kinetic constant (*k*) (Table 3) was larger for the emulsions than for CB (with $t_{1/2}$ values lower for emulsions than for bulk CB; data not shown). The values obtained for *k* together with the SFC curve shapes indicate that CB in emulsions crystallises faster than that in the bulk state.

To calculate the crystallisation parameters at 20 °C, the SFC data belonging to the linear region in a double logarithmic plot was used for the fitting, which corresponded to a holding time range between 35 and 65 min for emulsions. For CB containing 1% PGPR and bulk CB, the selected holding period corresponded to 45 and 75 min and 120 and 150 min, respectively, as these systems

displayed longer induction times. For all the systems, a good data fitting was obtained ($R^2 \geq 0.962$), and the Avrami exponent (n) had a value of 4 for all systems (Table 3). This value is in agreement with the data in the literature (Toro-Vazquez, Pérez-Martínez, Dibildox-Alvarado, Charó-Alonso, & Reyes-Hernández, 2004). A value of n of approximately 4 suggests a mechanism of heterogeneous nucleation from sporadic nuclei (Yang et al., 2013). Values of k (Table 3) were comparable among emulsions and CB containing 1% PGPR, whereas smaller values were obtained for bulk CB, thus quantifying the slower crystallisation process occurring in the latter.

While microstructural differences did not affect the kinetics of solidification at 5 °C and 10 °C, the results obtained at 15 °C and 20 °C suggested that emulsified CB crystallises faster than bulk CB. From the initial hypothesis, this behaviour can be explained by considering that water droplets act as seeds within the fat phase, thus accelerating the solidification process. However, the comparable n values for all systems at the four crystallisation temperatures suggest that the mechanism of crystallisation may have not been affected by the presence of dispersed droplets.

3.2.3. Polymorphic behaviour

In this section, the result of the deconvolution analysis of melting curves are discussed. This study aimed to gain an insight on polymorph developments as a function of crystallisation temperature and samples microstructure using mathematical treatment of DSC data.

3.2.3.1. Polymorphic evolution at 5 °C. Fig. 3 shows the average melting curves registered at 5 °C at all time points for the four CB systems. Analysis of the endotherms (Fig. 3) revealed some differences in the polymorphic evolution between bulk CB and emulsions. Although all samples had a main peak at approximately 20 °C in the first 20 min of crystallisation, suggesting the presence of an α form, a shoulder at approximately 25 °C was observed at an early stage only for emulsions. Moreover, for these systems, melting curves were centred at 25 °C after 30 min of annealing with the peak corresponding to a decrease in the α form over time. This was particularly evident for the 40% emulsion where an α form peak appeared as a small bump at the end of the experiment.
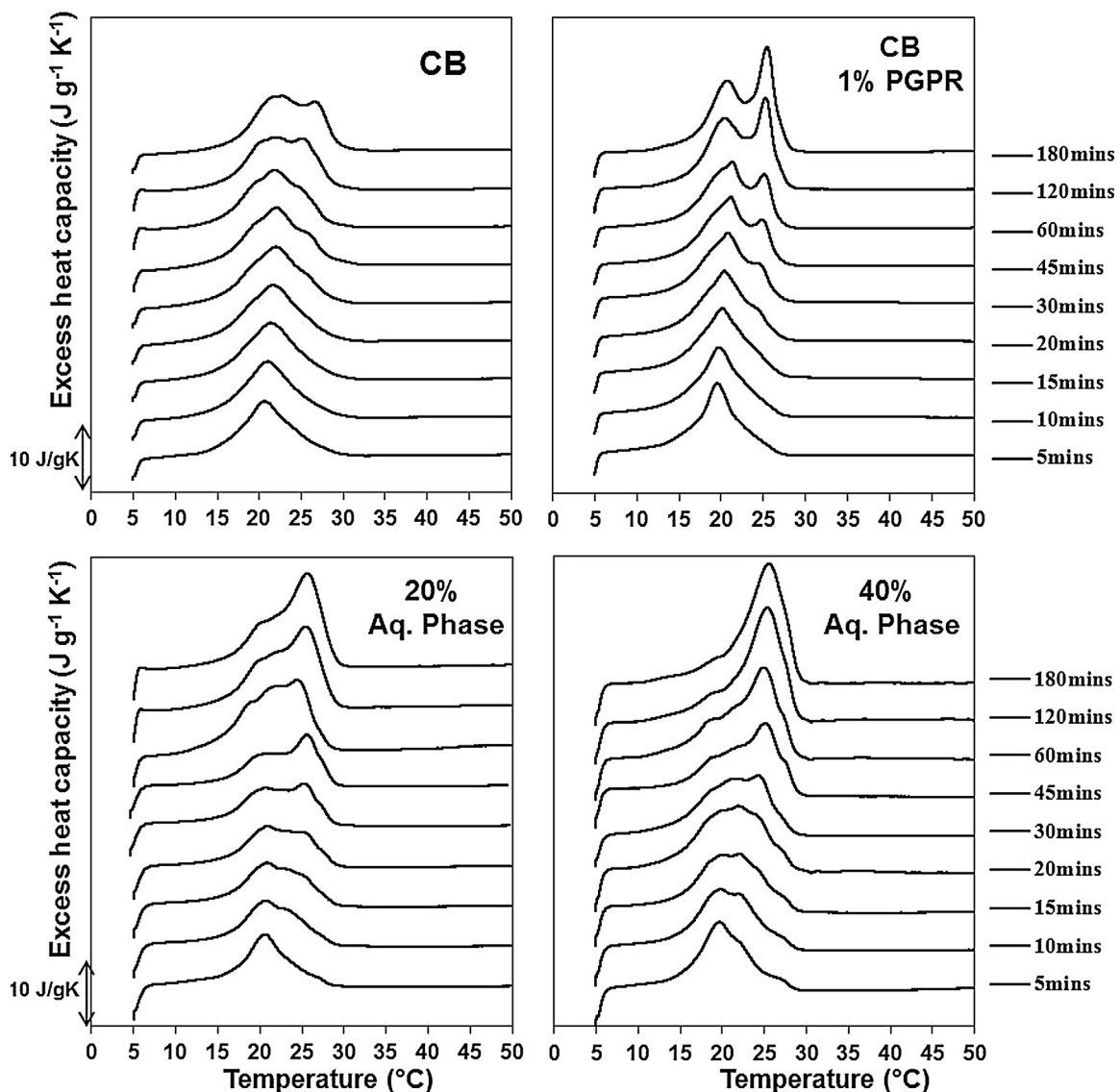

Fig. 3. Average melting curves for CB systems crystallised at 5 °C at all holding times. The time point corresponding to each melting curve and the CB system are referred in the figure.

For bulk CB, the main peak was obtained at approximately 23 °C, suggesting that it mostly remained in Form III. Nevertheless, the development of a second peak at approximately 26 °C was visible towards the end of the experiment, revealing the presence of Form IV. CB containing 1% PGPR showed the presence of two distinct peaks: the lower temperature peak was broader and smaller, whereas the higher temperature peak was sharp and high; these two peaks suggest a mixture of Form II and III and Form IV, respectively.

Results obtained from the deconvolution analysis of endotherms recorded at 5 °C are shown in Fig. 4. In each graph, the relative fraction (expressed in percentage) of each polymorph is shown as a function of the annealing time. After 5 min of crystallisation, all the systems were mainly in Form II (α polymorph). This result is expected as the α polymorph is the fastest form to crystallise according to the Ostwald step rule. This rule predicts that the least stable form (α) is the fastest to crystallise when crystallisation is induced by a temperature decrease. The α polymorph remained as the predominant form for the first 20 min for bulk CB and CB containing 1% PGPR. In the case of emulsions, Form III remained predominant until 30 min of crystallisation and was thereafter replaced by Form IV. As a general trend, Form IV grows at the expense of Form III, with the latter evolving from Form II. It should be considered that although in all the systems, the least stable α form represented approximately 20% of the solid phase after 60 min of crystallisation, Form IV became predominant (≥50%) only in the emulsions. Bulk CB and CB containing 1% PGPR remained mostly in Form III, with Form IV being approximately 40%. It is important to consider that as the equilibrium in the SFC value was reached after approximately

45 min of crystallisation (crystal fraction of approximately 0.9), the increase in the enthalpy values at longer annealing time (Fig. 2, panel at 5 °C) can be attributed to the polymorphic transition. This latter result is in agreement with that of Fessas et al. (2005) who reported that after the crystallisation was completed, the DSC signal was produced by the polymorphic transitions. Polymorphic behaviour at 10 °C (supplementary Image 3) was similar to that described for crystallisation at 5 °C. However, in the case of emulsions, the presence of Form V was detected towards the end of the annealing process.

3.2.3.2. Polymorphic evolution at 20 °C. Fig. 5 shows the average endotherms for all CB systems crystallised at 20 °C. In the first 15 min, peaks appear rather small and broad, revealing the presence of small amounts of crystalline material, which is consistent with SFC data (Fig. 1 panel at 20 °C). For both emulsified systems, the endotherm at 20 min appears broad, suggesting the presence of Form II, III and IV, with Form IV being predominant. For bulk CB and CB containing 1% PGPR, the endotherm at the same time point was also broad, but Form III appeared to be predominant. At a longer annealing time, a peak between 25 °C and 27 °C became clearly visible; this was the main peak at the end of the crystallisation period. A better understanding of the polymorphic evolution can be gained from the results of the deconvolution analysis (Fig. 6). To consider the contribution of the α form, following the melting range proposed by Van Malssen et al. (1999), the fusion point corresponding to this polymorph was centred at 22 °C. However, this implied that it was not possible to accurately signalling out the contribution associated with this form. Results (Fig. 6) indicate that Form III
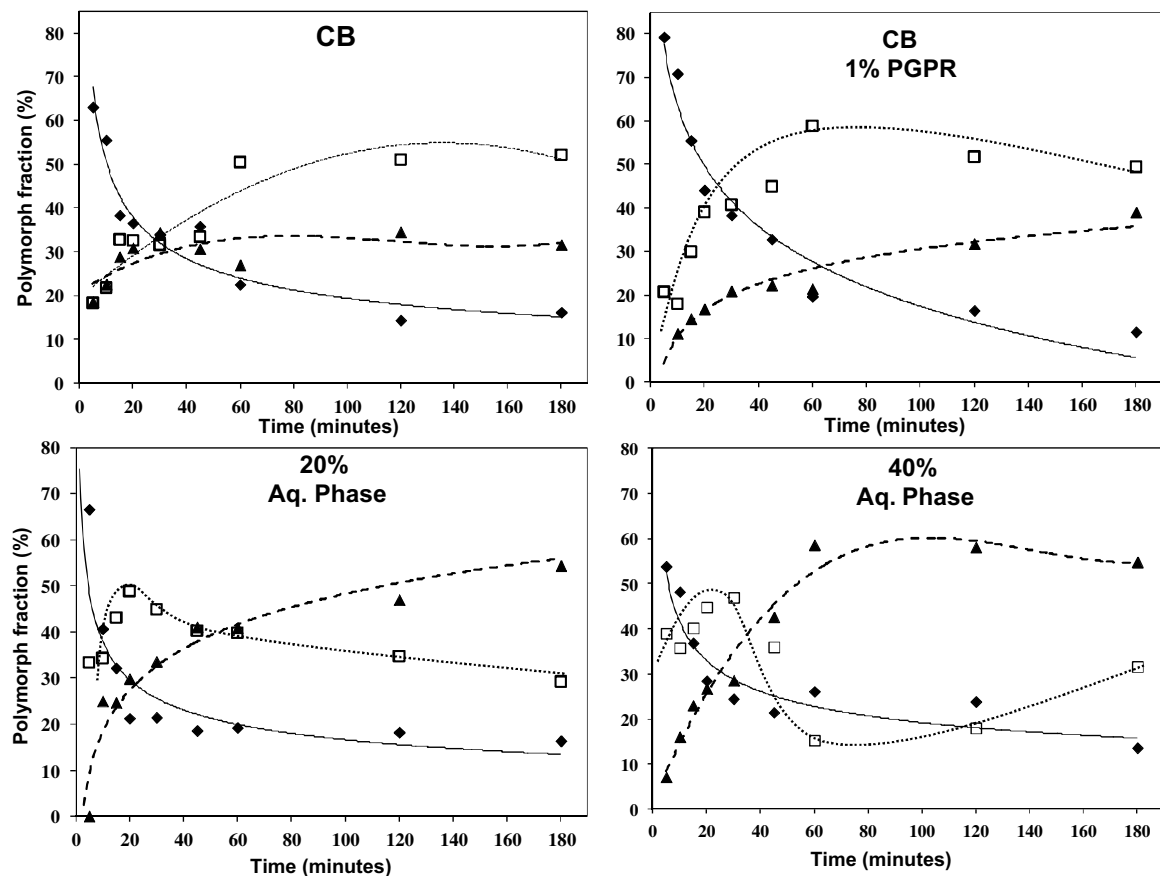

Fig. 4. Polymorphic evolution of CB systems crystallised at 5 °C. Form II, III, and IV are represented by diamond, square, and triangles, respectively. Lines serve only to guide the reader's eye: solid, dotted, and dashed lines correspond to Form II, III, and IV, respectively.
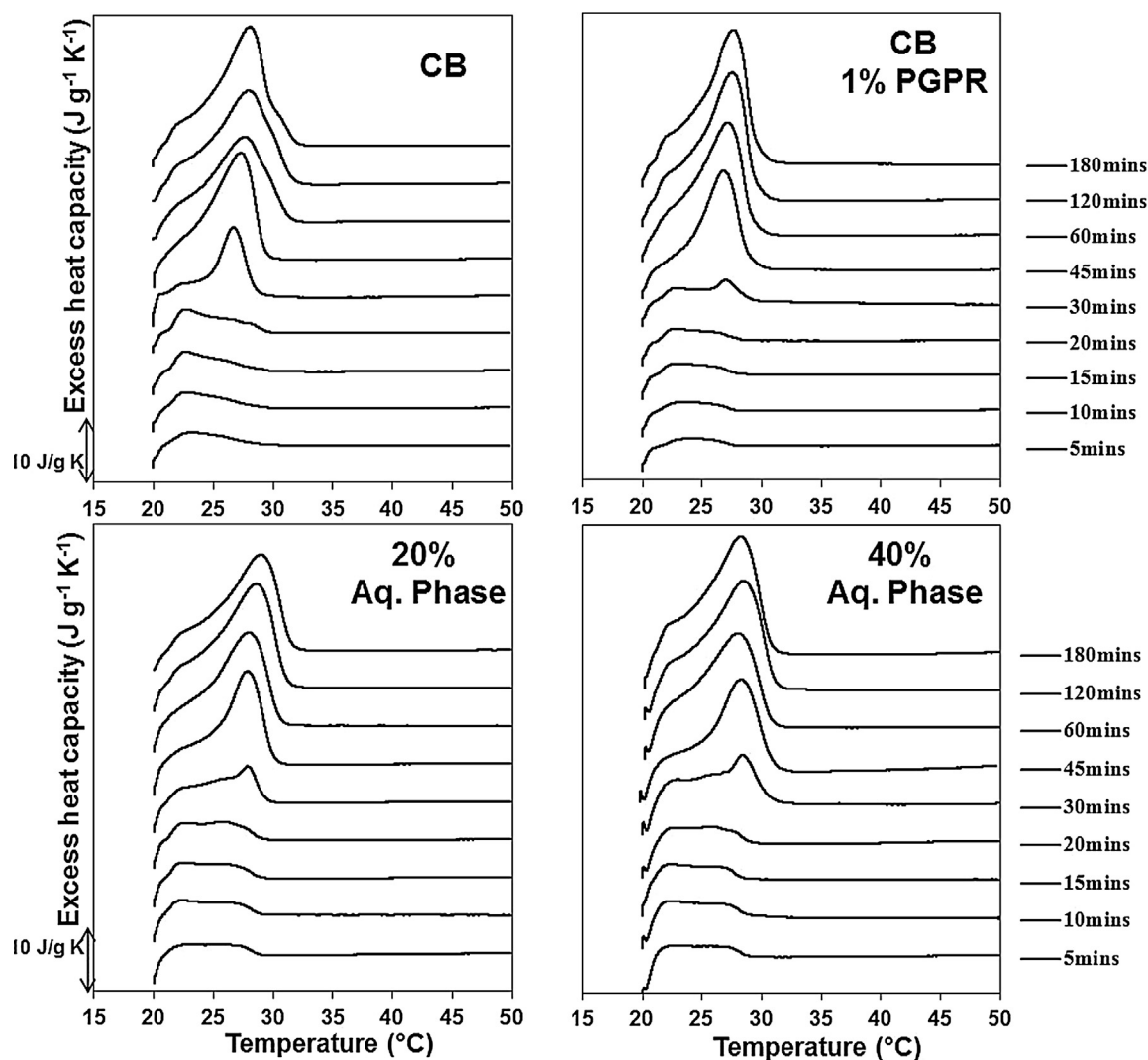
Fig. 5. Average endothermic curves for CB systems crystallised at 20 °C at all the selected holding times. The time point corresponding to each melting curve and the investigated system are referred in the figure.

was the major fraction at the beginning of the crystallisation in all CB systems, with Form II representing less than 20% of the total. At 30 min of annealing, Form IV became the predominant one in all systems. In bulk CB, it represented approximately 55%, with Form III and V accounting for 30% and 10% of the total, respectively, at the end of the crystallisation. In the case of emulsions, similar to that observed at 15 °C (supplementary Image 4), the development of Form IV was limited by the growth of Form V, suggesting a faster polymorphic transition. CB containing 1% PGPR showed the slowest polymorphic evolution, with Form III, IV and V representing 40%, 50% and 5% of the total, respectively. The possible mechanism of polymorphic evolution is described in Section 4.2.

4. Discussion

The shape of SFC curves and Avrami parameters provide information on the phase transition (type of nucleation and crystallisation rate are quantified by n and k, respectively) and crystal growth mechanism (n value at different temperatures) (Metin & Hartel, 1998; Marangoni and Mcgauley, 2003). SFC curves were used to identify the role of microstructure on the kinetics of crystallisation in CB systems. Microstructural changes were

produced by introducing seeds for crystallisation in the form of water droplets or by enriching the CB with the emulsifier. Deconvolution analysis of endotherms was used to compare polymorphic evolution among the systems.

4.1. Effect of water droplets on the kinetics of crystallisation

It is known that CB contains impurities in the form of complex lipids (glycolipids and phospholipids) and saturated TAGs (Davis & Dimick, 1989). These lipids form high-melting point crystals that partially phase-separate from the monounsaturated TAGs fraction and seed CB crystallisation (Loisel, Keller, Lecq, Bourgaux, & Ollivon, 1998). Therefore, it can be assumed that in all the systems investigated in this study, nucleation occurred through a heterogeneous route, and emulsions simply contained a larger number of 'crystallisation seeds'.

Results suggest that no difference in the crystallisation kinetics occurs when CB systems are rapidly supercooled to 5 °C or 10 °C: all curves have approximately a hyperbolic shape with no induction time. The n value of approximately 1 suggests an instantaneous nucleation mechanism, which implies that all nuclei are formed at the beginning of the crystallisation once the crystallisation temperature is reached. The type of nucleation and absence of
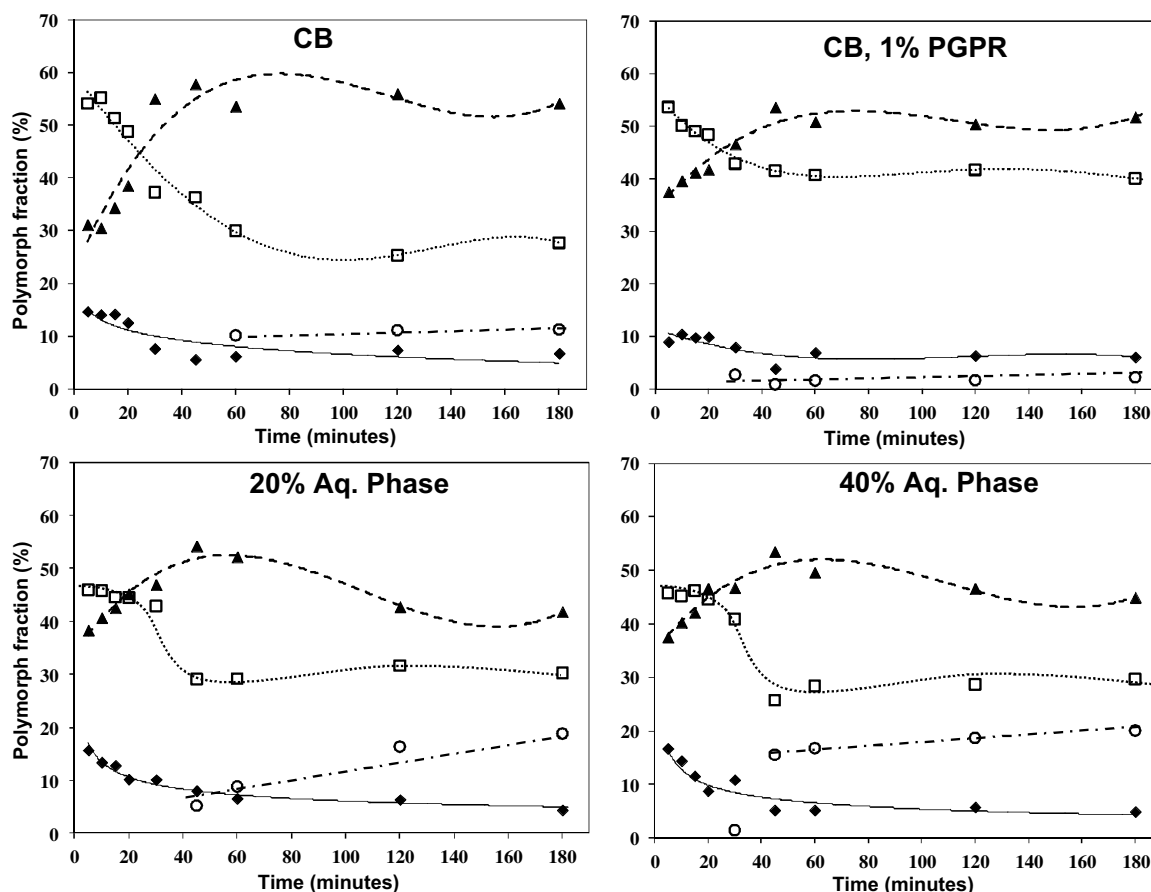
Fig. 6. Polymorphic evolution of CB systems crystallised at 20 °C. Form II, III, IV, and V are represented by diamond, square, triangles, and circles, respectively. Lines serve only to guide the reader's eye: solid, dotted, dashed, and dashed-dotted line is for Form II, III, IV, and V, respectively.

differences among systems can be explained by the degree of supercooling inducing fast nucleation, which masks the seeding effect provided by water droplets. This result is in line with the theoretical description reported in the literature (Sato & Ueno, 2011).

Results at 15 °C revealed some differences in the crystallisation behaviour of the systems. The values of kinetic constant k measured for emulsions were higher than those for CB, suggesting a faster transformation. The Avrami exponent (n) had a value of 2 in all the systems. Metin and Hartlel (1998) reported that such value indicates a process characterised by a high initial nucleation rate (*instantaneous nucleation*) and plate-like crystal growth. Here, although crystal morphology was not studied, considering the degree of supercooling (approximately 25 °C), it is reasonable to assume that the presence of droplets accelerates the crystallisation process compared to bulk CB, with the mechanism of crystallisation remaining the same across systems.

As indicated by the values of k at 20 °C, emulsions crystallised faster than in bulk CB (Table 3), but no difference in the Avrami exponent was detected. The increase in the n value to approximately 4 indicates a process of sporadic nucleation, i.e. the number of nuclei linearly increased with time (Yang et al., 2013). It also suggests that crystal growth evolves from a one- to a multidimensional phenomenon (Wright, Hartel, Narine, & Marangoni, 2000). The considerably longer induction time observed for bulk CB indicates that the fat phase required longer time to form stable nuclei. CB containing 1% PGPR showed similar crystallisation behaviour to emulsions. It is possible that emulsifier molecules may self-structure in the melt and act as seeds for crystallisation. These results suggest that a crystallisation kinetics are

considerably increased by only a small number of nuclei and do not scale with seeds number. From the obtained results, it can be concluded that emulsified water droplets structured within the fat matrix act as catalytic impurities, promoting an overall faster crystallisation process than in bulk CB.

4.2. Effect of water droplets on polymorphic evolution

Results of the deconvolution analysis revealed a complex polymorphic evolution for all CB systems, with emulsions characterised by a larger fraction of stable polymorphs at all temperatures. From literature data (Loisel et al., 1998; Lopez et al., 2001), it is reasonable to assume that the first fraction to crystallise is represented by trisaturated TAGs arranged in α conformation. The monounsaturated TAGs, the main CB lipid fraction (≥80%, wt %), crystallises at around 15 °C in a complex crystalline arrangement.

With respect to polymorphic evolution, data shown in Section 3.2.3.1 suggest that at a crystallisation temperature of 5 °C or 10 °C, the α form, which crystallises the fastest, is always predominant at an early stage of the solidification process. This is in agreement with the Ostwald step rule, i.e. the polymorph with the lowest activation energy of nucleation is the fastest to crystallise, and with literature data (Marangoni & Mcgauley, 2003). At crystallisation temperature of 15 °C and 20 °C, the α form was not found to be the predominant one, with the result attributed to the limit of the DSC and deconvolution technique.

For crystallisation temperature of 5 °C, 10 °C and 15 °C, the deconvolution analysis highlighted a complex pattern of polymorphic evolution occurring prior and after SFC had entered the

plateau region. The data indicate that for all systems, Form III grows at the expense of the α polymorph and evolves into Form IV. Moreover, Form II (α) to III transformation occurs simultaneously with further TAG crystallisation from the melt into the α form, given the high level of imposed supercooling ($\geq 25\,°C$) and its low activation energy of nucleation. Therefore, a mechanism of direct crystallisation from melt to Form III by heterogeneous crystallisation (templating) promoted by the presence of solid material in this conformation can be excluded. Evolution towards Form IV occurred after ($T_{Cr} = 5\,°C$ and $10\,°C$) or before ($T_{Cr} = 15\,°C$) the SFC had reached its maximum (curves in the plateau region). In agreement with Fessas et al. (2005), this result confirms that polymorphic evolution is a dynamic process and implies a continuous and gradual transformation from the less to the more stable forms. At these crystallisation temperatures, only in emulsified systems Form V could be detected. These results strongly suggest that CB in an emulsified state tends to evolve faster to more stable polymorphs. This is particularly relevant because Marangoni and Mcgauley (2003) stated that CB would remain stable in β′ form for 28 days at 15 °C. Here it was found that in emulsified CB, a transition to β form begins to occur within 2 h.

To explain the polymorphic evolution at 20 °C, a mechanism similar to that reported by Toro-Vazquez et al. (2004) could be hypothesised. These authors considered that the β′ polymorph can be formed either from α crystals or from the melt, depending on the time–temperature combination. At a crystallisation temperature of 20 °C, a small fraction of CB crystallises in the α form that evolves to β′ through a solid state transformation with further crystallisation occurring by heterogeneous templating nucleation into β′ form. Here, the α polymorph had probably been the first to crystallise, with evolution to Form III occurring prior/during reheating so that Form III appeared as the main polymorph on remelting. At longer times, the fraction of Form III increased as solidification of CB occurred directly in this form and (after 30 min of annealing) decreased because of Form IV growth, suggesting a direct $β′_2$ to $β′_1$ evolution. This transformation is in agreement with that described by Fessas et al. (2005). Our results are also in agreement with those reported by Marangoni and Mcgauley (2003) who showed that the crystallisation of β′ polymorph directly from the melt yielded an n value of ≥ 3.

To explain the faster polymorphic evolution observed in emulsions than in bulk CB and CB containing 1% PGPR, the molecular interfacial arrangement should be considered. Water droplets are covered by PGPR, which forms a non-elastic interface providing stability by steric interactions (Gülseren & Corredig, 2012). Because PGPR cannot co-crystallise with CB TAGs at the investigated temperatures, a liquid layer consisting of PGPR molecules is expected to exist surrounding the droplets, with the hydrophilic head interacting with the water and the tails pointing towards the lipid phase. This implies that PGPR molecules, although liquid, are partially ordered and can interact with TAGs of CB given some structural similarities of the acyl chain. It has been reported that PGPR molecules act as bridges between fat crystals and water, implicitly assuming a certain molecular interaction (Garti, Aserin, Tiunova, & Binyamin, 1999). The hypothesis of the existence of molecular interaction near droplet interfaces is also in agreement with recent findings suggesting that fat crystals close to the droplet interface have their lamellar planes aligned almost parallel to the plane of droplet interface (Wassell et al., 2012). This result was attributed by the authors to the hydrophobic interactions between fatty chains of PGPR and TAGs and hydrophilic interactions between PGPR and TAG glycerol groups. In a study on the crystallisation of CB, Loisel et al. (1998) investigated the fat crystallisation behaviour on cooling (and reheating) from 40 °C to 0 °C at 2 °C/min; the authors concluded that the α form is the first to crystallise and co-exists with liquid

crystals where the saturated chains of the TAGs create organised domains and the unsaturated molecules remain liquid-like. We hypothesise that within the temperature range investigated in this study (5 °C–20 °C), the CB triacylglycerol matrix initially consists of a solid–liquid mixture of the α form and liquid crystals (structures partially crystallised with the saturated chains forming organised solid domains and the unsaturated chain remaining liquid-like). Given some structural similarities, the unsaturated chain of the TAG liquid crystals may interact with the ricinoleic groups of PGPR. Moreover, α crystals are the most surface-active crystals (Johansson & Bergenståhl, 1995a, 1995b) because these crystals are characterised by an amorphous structure, with the aliphatic chains oscillating and characterised by a high degree of freedom (Timms, 1984). Therefore, it seems reasonable to hypothesise an interaction near the interface between PGPR molecules and CB TAG crystals both in the α form and in a liquid crystal state. It can be speculated that the interaction between these liquid moieties would promote structural re-arrangements of TAG molecules, which would result in enhanced polymorphic transition. The presence of a liquid phase promotes polymorphic evolution towards more stable forms (Timms, 1984). The process hypothesised here is similar to that referred for CB enriched with 25% miglyol (Lopez et al., 2001) or 5% trilinolein (Campos, Ollivon, & Marangoni, 2010) (both in liquid form). In both cases, the authors concluded that the liquid fatty acid chains (within the network or at the crystal surfaces) would accelerate polymorphic transformation by increasing the molecular re-arrangement and diffusion, thus allowing more stable conformations to be formed. In the present study, PGPR chains protruding from droplet interface would interact with TAG molecules, thus increasing their molecular mobility and structural re-arrangement, which results in the development of more stable forms. The evidence that CB containing 1% PGPR is characterised by a polymorphic evolution that is comparable to or slower than bulk CB further supports the hypothesis that an interfacial local ordering at the droplet interface is required for accelerating the polymorphic transition.

5. Conclusions

The results of the SFC analysis and data from the kinetic analysis have highlighted the differences in the crystallisation behaviour of CB depending on its physical state. When existing as the continuous phase of an emulsion for $T_{Cr} \geq 15\,°C$, CB in emulsions evolved faster (higher value of k) towards the equilibrium SFC than bulk CB. The similarity in the values of the Avrami exponent (n) among the systems at all temperatures suggests that the crystallisation mechanisms are not affected by microstructural changes. Furthermore, the increase to $n = 4$ at 20 °C suggests a change in the dimensions of crystal growth (from mono- to multidimensional) and, possibly, in the crystallisation of Form III directly from the melt, similar to that observed in milk fat (Wright et al., 2000).

In CB system polymorphism, the deconvolution analysis of a large number of DSC curves permitted the understanding of polymorphic evolution depending on the CB physical structure. Within the investigated temperature range, in all samples, CB crystallised in the metastable forms of α (II) and $β′_2$ (III) (at 20 °C) at an early stage of the annealing process. Emulsified CB evolved more quickly towards more stable forms, and a significant fraction of Form V was detected towards the end of the resting period. This result was explained using the hypothesis of a mechanism of 'facilitated TAG structural re-arrangement' near the interface: the presence of partially organised liquid PGPR moieties and CB TAGs in the α form (and, by speculation, also of liquid crystals) at the water interface enhances molecular mobility and structural re-arrangement, thus increasing polymorphic evolution (similar to

that occurring in a melt-mediated polymorphic transformation). Furthermore, the evidence that a CB system containing 1% PGPR did not exhibit any difference in terms of polymorphic evolution compared to bulk CB suggests that a certain degree of ordering (here provided by the interface) may be necessary to increase polymorphic transformation.

Acknowledgement

Appendix A. Supplementary data

Supplementary data associated with this article can be found, in the online version, at http://dx.doi.org/10.1016/j.foostr.2016.10.001.

References

Arima, S., Ueno, S., Ogawa, A., & Sato, K. (2009). Scanning microbeam small-angle x-ray diffraction study of interfacial heterogeneous crystallization of fat crystals in oil-in-water emulsion droplets. *Langmuir*, *25*, 9777–9784.

Bayés-García, L., Patel, A. R., Dewettinck, K., Rousseau, D., Sato, K., & Ueno, S. (2015). Lipid crystallization kinetics—Roles of external factors influencing functionality of end products. *Current Opinion in Food Science*, *4*, 32–38.

Campos, R., Ollivon, M., & Marangoni, A. G. (2010). Molecular composition dynamics and structure of cocoa butter. *Crystal Growth & Design*, *10*, 205–217.

Davis, T. R., & Dimick, P. S. (1989). Isolation and thermal characterization of high-melting seed crystals formed during cocoa butter solidification. *Journal of the American Oil Chemists Society*, *66*, 1488–1493.

Dewettinck, K., Foubert, I., Basiura, M., & Goderis, B. (2004). Phase behavior of cocoa butter in a two-step isothermal crystallization. *Crystal Growth & Design*, *4*, 1295–1302.

Di Bari, V., Norton, J. E., & Norton, I. T. (2014). Effect of processing on the microstructural properties of water-in-cocoa butter emulsions. *Journal of Food Engineering*, *122*, 8–14.

Di Bari, V. (2015). *Large deformation and crystallisation properties of process optimised cocoa butter emulsions*. University of Birmingham [PhD Thesis].

Douaire, M., Di Bari, V., Norton, J. E., Sullo, A., Lillford, P., & Norton, I. T. (2014). Fat crystallisation at oil–water interfaces. *Advances in Colloid and Interface Science*, *203*, 1–10.

Fessas, D., Signorelli, M., & Schiraldi, A. (2005). Polymorphous transitions in cocoa butter. *Journal of Thermal Analysis and Calorimetry*, *82*, 691–702.

Foubert, I., Vanrolleghem, P. A., & Dewettinck, K. (2003). A differential scanning calorimetry method to determine the isothermal crystallization kinetics of cocoa butter. *Thermochimica Acta*, *400*, 131–142.

Foubert, I., Vanrolleghem, P. A., & Dewettinck, K. (2005). Insight in model parameters by studying temperature influence on isothermal cocoa butter crystallization. *European Journal of Lipid Science and Technology*, *107*, 660–672.

Foubert, I., Fredrick, E., Vereecken, J., Sichien, M., & Dewettinck, K. (2008). Stop-and-return DSC method to study fat crystallization. *Thermochimica Acta*, *471*, 7–13.

Fredrick, E., Van DE Walle, D., Walstra, P., Zijtveld, J. H., Fischer, S., Van Der Meeren, P., et al. (2011). Isothermal crystallization behaviour of milk fat in bulk and emulsified state. *International Dairy Journal*, *21*, 685–695.

Gülseren, & Corredig, M. (2012). Interactions at the interface between hydrophobic and hydrophilic emulsifiers: Polyglycerol polyricinoleate (PGPR) and milk proteins, studied by drop shape tensiometry. *Food Hydrocolloids*, *29*, 193–198.

Garti, N., Aserin, A., Tiunova, I., & Binyamin, H. (1999). Double emulsions of water-in-oil-in-water stabilized by α-form fat microcrystals. Part 1: Selection of emulsifiers and fat microcrystalline particles. *Journal of the American Oil Chemist' Society*, *76*, 383–389.

Ghosh, S., & Rousseau, D. (2011). Fat crystals and water-in-oil emulsion stability. *Current Opinion in Colloid & Interface Science*, *16*, 421–431.

Johansson, D., & Bergenståhl, B. (1995a). Sintering of fat crystal networks in oil during post-crystallization processes. *Journal of the American Oil Chemists' Society*, *72*, 911–920.

Johansson, D., & Bergenståhl, B. (1995b). Wetting of fat crystals by triglyceride oil and water. 2. Adhesion to the oil/water interface. *Journal of the American Oil Chemists' Society*, *72*, 933–938.

Loisel, C., Keller, G., Lecq, G., Bourgaux, C., & Ollivon, M. (1998). Phase transitions and polymorphism of cocoa butter. *Journal of the American Oil Chemists' Society*, *75*, 425–439.

Lopez, C., Riaublanc, A., Lesieur, P., Bourgaux, C., Keller, G., & Ollivon, M. (2001). Definition of a model fat for crystallization-in-emulsion studies. *Journal of the American Oil Chemists' Society*, *78*, 1233–1244.

Marangoni, A. G., & Mcgauley, S. E. (2003). Relationship between crystallization behavior and structure in cocoa butter. *Crystal Growth & Design*, *3*, 95–108.

Metin, S., & Hartel, R. W. (1998). Thermal analysis of isothermal crystallization kinetics in blends of cocoa butter with milk fat or milk fat fractions. *Journal of the American Oil Chemists' Society*, *75*, 1617–1624.

Norton, J. E., & Fryer, P. J. (2012). Investigation of changes in formulation and processing parameters on the physical properties of cocoa butter emulsions. *Journal of Food Engineering*, *113*, 329–336.

Norton, J. E., Fryer, P. J., Parkinson, J., & Cox, P. W. (2009). Development and characterisation of tempered cocoa butter emulsions containing up to 60% water. *Journal of Food Engineering*, *95*, 172–178.

Oliver, L., Scholten, E., & Van Aken, G. A. (2015). Effect of fat hardness on large deformation rheology of emulsion-filled gels. *Food Hydrocolloids*, *43*, 299–310.

Pérez-Martínez, D., Alvarez-Salas, C., Charó-Alonso, M., Dibildox-Alvarado, E., & Toro-Vazquez, J. F. (2007). The cooling rate effect on the microstructure and rheological properties of blends of cocoa butter with vegetable oils. *Food Research International*, *40*, 47–62.

Rivas, J. C. M., Zelga, K., Schneider, Y., & Rohm, H. (2016). Phase transition stability of cocoa butter emulsions. *Food Biophysics*, *11*, 361–369.

Rousseau, D., Ghosh, S., & Park, H. (2009). Comparison of the dispersed phase coalescence mechanisms in different tablespreads. *Journal of Food Science*, *74*, E1–E7.

Rousseau, D. (2013). Trends in structuring edible emulsions with Pickering fat crystals. *Current Opinion in Colloid & Interface Science*, *18*, 283–291.

Sato, K., & Ueno, S. (2011). Crystallization: Transformation and microstructures of polymorphic fats in colloidal dispersion states. *Current Opinion in Colloid & Interface Science*, *16*, 384–390.

Sullo, A., Arellano, M., & Norton, I. T. (2014). Formulation engineering of water in cocoa – Butter emulsion. *Journal of Food Engineering*, *142*, 100–110.

Timms, R. E. (1984). Phase behaviour of fats and their mixtures. *Progress in Lipid Research*, *23*, 1–38.

Toro-Vazquez, J. F., Pérez-Martínez, D., Dibildox-Alvarado, E., Charó-Alonso, M., & Reyes-Hernández, J. (2004). Rheometry and polymorphism of cocoa butter during crystallization under static and stirring conditions. *Journal of the American Oil Chemists' Society*, *81*, 195–202.

Ueno, S., Hamada, Y., & Sato, K. (2003). Controlling polymorphic crystallization of n-alkane crystals in emulsion droplets through interfacial heterogeneous nucleation. *Crystal Growth & Design*, *3*, 935–939.

Van Malssen, K., Van Langevelde, A., Peschar, R., & Schenk, H. (1999). Phase behavior and extended phase scheme of static cocoa butter investigated with real-time X-ray powder diffraction. *Journal of the American Oil Chemists' Society*, *76*, 669–676.

Van Putte, K., & Van Den Enden, J. (1974). Fully automated determination of solid fat content by pulsed NMR. *Journal of the American Oil Chemists Society*, *51*, 316–320.

Wassell, P., Okamura, A., Young, N. W. G., Bonwick, G., Smith, C., Sato, K., et al. (2012). Synchrotron radiation macrobeam and microbeam x-ray diffraction studies of interfacial crystallization of fats in water-in-oil emulsions. *Langmuir*, *28*, 5539–5547.

Wright, A. J., Hartel, R. W., Narine, S. S., & Marangoni, A. G. (2000). The effect of minor components on milk fat crystallization. *Journal of the American Oil Chemists' Society*, *77*, 463–475.

Yang, D., Hrymak, A. N., & Kedzior, S. (2013). Kinetics of isothermal crystallization of hydrogenated castor oil-in-water emulsions. *Journal of the American Oil Chemists' Society*, *90*, 1743–1750.